Theoretical analysis of a regenerative supercritical carbon dioxide Brayton cycle/organic Rankine cycle dual loop for waste heat recovery of a diesel/natural gas dual-fuel engine

Youcai Liang[1, 2], Xingyan Bian[1], Weiwei Qian[1], Mingzhang Pan[1]*, Zhibo Ban[3], Zhibin Yu[2]

1 Guangxi Key Laboratory of Manufacturing System & Advanced Manufacturing Technology, School of of Mechanical Engineering, Guangxi University, Nanning 530004, China

2 Systems, Power & Energy Research Division, School of Engineering, University of Glasgow, Glasgow G12 8QQ, UK

3 Advanced Technology Center, Research and Engeering Institute, Guangxi Yuchai Machinery CO.Ltd

[*] Corresponding author: E-mail address: pmz@gxu.edu.cn

ABSTRACT: Supercritical carbon dioxide Brayton cycle is considered one of the most promising systems for waste heat recovery of engines because of its compactness and high energy efficiency. To further improve the fuel utilization ratio and solve the difficulties of waste heat recovery of high temperature exhaust gas, a regenerative supercritical carbon dioxide Brayton cycle/organic Rankine cycle dual loop is proposed for cascade utilization of exhaust heat from a dual-fuel engine. The regenerative supercritical carbon dioxide Brayton cycle of the proposed system is powered by the waste heat contained in the exhaust gas. The working fluid in the organic Rankine cycle is pre-heated by CO_2 exiting the regenerator and then further heated by the residual heat of the exhaust gas. The flow rates of the working fluids in both sub cycles are adjusted to match the waste heat recovery system to respond to the changing conditions of the dual-fuel engine. The results revealed that the maximum net power output of this system is up to 40.88 kW, thus improving the dual-fuel engine power output by 6.78%.

Therefore, such a regenerative supercritical carbon dioxide Brayton cycle/organic Rankine cycle dual loop system design enables the thorough recovery of high temperature exhaust heat, leading to higher energy efficiency and lower fuel consumption of the engine.

Key words: Supercritical carbon dioxide Brayton cycle; Organic Rankine cycle; Dual-fuel engine; Waste heat recovery; Thermodynamic performance

Introduction

The increased prominence of the energy crisis and environmental pollution problems, has led to the search for solutions such as finding alternative fuels or improving fuel utilization ratio. For the former, hydrogen, which can be produced from biomass gasification effectively [1], has immense potential for application. For the latter, engines as one of the main consumers of fuel have attained extensive attention. In terms of dual-fuel engines, approximately 30%–45% of fuel energy is converted into useful work, while the remaining energy is released into the atmosphere in the form of heat through exhaust gases, jacket water, and lubrication oil. Generally, there are two ways to improve energy efficiency of a dual-fuel engine: The first is to optimize the internal structure and combustion process of the dual-fuel engine, and the other is to capture and reclaim waste heat. As structure and combustion technologies have been optimized to their best potential, it becomes harder to achieve further improvement using these methods. In contrast, the high temperature of the exhaust gas makes waste heat recovery

(WHR) one of the best energy saving technologies for more efficient fuel usage to help improve the environment.

Recently, WHR of engine has been studied widely by both experiment and simulation. The organic Rankine cycle (ORC) has immense applicability because of its capability for low temperature heat recovery, compactness, and low erosion. Studies on ORC have focused on various factors that affect its performance, such as selection of organic working fluids, optimization of cycle parameters, and comparison among different layouts. Thurairaja et al. [2] and Scaccabaraozee et al. [3] analyzed the suitable scopes of different organic working fluids to achieve the best match between organic working fluids and working conditions. Additionally, Abadi et al. [4] summarized the advantages and issues of using zeotropic mixtures in ORC and the results showed that in comparison with pure fluids, zeotropic mixtures would increase exergy efficiency by decreasing the irreversibility in the heat exchangers. Braimakis et al. [5] confirmed that adding a regenerator can improve ORC efficiency. Moreover, BMW proposed the dual-loop cycle (called turbosteamer cycle) driven with a 1.8-liter BMW four-cylinder to achieve higher energy efficiency [6]. To find a better match and reduce the temperature difference between the working fluid and the heat source, supercritical and transcritical ORCs were proposed in the WHR area because they did not undergo liquid-gas phase transition in heat exchangers. Li et al. [7] studied the performance of subcritical and transcritical ORCs using R1234ze driven by 100-200 °C hot water. Results showed that transcritical ORC showed higher system efficiency and was suitable for higher temperatures compared with subcritical ORC. Mohammadkhani et al. [8] adopted a transcritical dual loop ORC to recover the waste heat of diesel engines. The results showed that the best performance was achieved using toluene and R143a in the high and low-temperature loops, respectively. At the same time, supercritical ORC has been rapidly developed because of its lower exergy loss and higher energy efficiency. The effect of condensation temperature [9] and organic working fluids [10] on supercritical ORC had been investigated. Moreover, Moloney et al. [11] presented a parametric analysis of a regenerative supercritical ORC. Braimakis et al. [12] compared supercritical and transcritical ORCs with different working fluids. Results showed that supercritical ORC in mixtures exhibited better thermodynamic performance for temperatures above 170 °C. In diesel/natural gas dual-fuel engines, the maximum temperature of the exhaust gas approximately ranges from 720 to 870 K when they are operated under a medium/high operating load [13], while the decomposition temperatures of most working fluids are below 600 K. On account of the decomposition issue of organic working fluids, ORC application is limited in the field of engine WHR. Furthermore, the size and weight of the turbine need to be considered, because of which ORC has not been applied in automobile engine WHR although it has been investigated and tested for a long time. The supercritical carbon dioxide Brayton cycle (SCBC) was proposed by Fether [14] and Angelino [15] because carbon dioxide is environment friendly and noninflammable and has good chemical stability, a low critical point, high specific heat capacity, and high heat transfer efficiency. As the performance of heat exchangers and turbines has improved, the SCBC, which is more suitable for high temperature WHR than supercritical ORC, has gradually become a hotspot of research.

Various SCBC layouts were proposed in the past two decades. Crespi et al. [16] organized the numerous cycles in different categories and compared the claimed performance of each cycle. Li et al. [17] presented the advantages and classifications of SCBCs and theoretically and experimentally analyzed their application in various industries. Zhu et al. [18] compared different direct-heated SCBCs integrated with a solar thermal power tower system. Results showed that the intercooling SCBC achieved the highest overall efficiency. Sarkar [19] explored the effects of cycle parameters on supercritical carbon dioxide recompression Brayton cycle (SCRBC) and found that the irreversibility of heat exchangers was much higher than that of the turbomachinery. Kim et al. [20] focused on the influence of pinch point temperature difference on the irreversibility of heat exchangers and cycle efficiency. Park et al. [21] analyzed the application of SCRBC in various small reactors and investigated the effects of channel shape of printed circuit heat exchangers (PCHEs) on pressure drop. They proved that using airfoil fin type PCHE may increase the thermal efficiency by about 1.0% in comparison with zigzag type PCHE. Although the layouts, operating parameters, and components of simple SCBC had been optimized, its energy efficiency is relatively low due to the high temperature of carbon dioxide entering the cooler. Therefore, multi-loop layouts have been adopted to take full advantage of the remaining energy to raise specific power. Manente et al. [22] studied the application of cascaded SCBCs in biomass. The results revealed that a maximum biomass to electricity conversion efficiency of 36% can be achieved by the cascaded configuration, which was 4.7% higher than that of the simple cascaded system using the same boiler design. Wang et al. [23] indicated that the total product unit cost of SCBC/ORC was slightly lower than that of supercritical carbon dioxide Brayton cycle/transcritical carbon dioxide Brayton cycle (SCBC/TCBC). Exergoeconomic analysis and optimization of SCRBC/ORC were made by Akbari [24]. The results indicated that the highest exergy efficiency and the lowest product unit cost for SCRBC/ORC were obtained when Isobutane and RC318 were used as the ORC working fluids, respectively. Singh et al.[25] comprehensively analyzed the energy and exergy of SCBC/ORC combined cycle driving solar parabolic trough collectors and showed that R407c combined cycle obtained the maximum exergy and energy efficiency.

With the maturity of SCBC, some scholars and companies attempted to apply it to engine WHR in recent years. Song et al. [26] adopted a preheating SCBC to recover jacket cooling water and the waste heat of a diesel engine. The findings showed that the improved preheating SCBC based system for WHR increased the engine power output by 6.9%. The performance of regenerative SCBC (RSCBC)/ORC and SCRBC/ORC was discussed and analyzed [27]. Uusitalo et al. [28] investigated the electricity production potential of SCBCs for engine WHR with different operational conditions and working fluids. They concluded that the working fluids and cycle operational parameters not only significantly influenced the thermodynamic cycle design but also highly affected the optimal rotational speed and geometry of the turbomachines. Several studies focused on SCBC for engine WHR, however, a diesel engine was used to explore the effect of a single parameter on cycle performance under a single engine condition. Due to the high temperature exhaust gas of diesel/natural gas dual-fuel engine, no study has focused on its WHR. In this study, a novel RSCBC/ORC dual loop cycle is proposed and discussed for WHR of a diesel/natural gas dual-fuel engine, which has been shown to be a more potential system for its better thermodynamic performance compared with RSCBC and its excellent thermal stability compared with ORC. The design of such a dual loop cycle enables not only the cascade utilization of the waste heat of the dual-fuel engine but also the thorough use of the residual heat of the high temperature cycle (HT cycle). Moreover, the energy and exergy of this dual loop cycle under different working conditions of the dual-fuel engine are assessed to better match the changing conditions of the dual-fuel engine, which can provide reference for its practical application and design of control system. The optimization of multiple parameters and the selection of organic working fluids are also discussed.

2. System description

YC6MK375DN is selected as the dual-fuel engine in this study. The speed of the engine was kept constant at 1500 rpm, while its load was varied under different conditions. Four different conditions were considered, and the main parameters are shown in Table 1. Under the assumption that the dual-fuel engine burns completely, the exhaust gas is mainly assumed to be composed of N_2, CO_2, H_2O, and O_2. The mass percentage of each of component is calculated using the chemical reaction equation of complete combustion, as shown in Table 2. Next, the specific heat capacity and enthalpy of the exhaust gas can be obtained by REFPROP. In this study, natural gas and diesel are simplified to pure methane (CH_4) and $C_{12}H_{23}$, respectively. Their complete reaction equation can be expressed as follows:

$$CH_4 + 2(O_2 + 3.773N_2) = CO_2 + 2H_2O + 7.546N_2 \quad (1)$$

$$C_{12}H_{23} + 17.75(O_2 + 3.773N_2) = 12CO_2 + 11.5H_2O + 66.97N_2 \quad (2)$$

Table 1 Main parameters of the dual-fuel engine

Torque (N·m)	800	1200	1400	1600
Engine power output (kW)	126.8	189	220.8	251.1
Engine efficiency (%)	34.0	38.9	40.7	41.6
Exhaust temperature (℃)	423.2	452.3	463.8	488.3
Exhaust mass flow rate (kg/h)	825	1006	1074	1139

Table 2 Composition of the exhaust gas

Torque (N·m)	N_2 (%)	H_2O (%)	CO_2 (%)	O_2 (%)
800	74.29	6.97	9.08	9.66
1200	74.11	7.47	9.59	8.83
1400	73.98	7.87	10.04	8.11
1600	73.85	8.25	10.48	7.42

A schematic diagram of the WHR system is shown in Fig. 1. The system consists of a RSCBC and an ORC with a pre-heater. The RSCBC is composed of a compressor, heater, turbine, regenerator, and cooler. The CO_2 exiting from the compressor is heated by the regenerator and heater in series. The high temperature S-CO_2 stream expands in the turbine, and the high temperature expanded stream heats the compressed S-CO_2 and organic working fluid in series and then returns to the cooler. In ORC, the organic working fluid at the outlet of the pump is pre-heated by the residual heat of CO_2 exiting from the regenerator and then is further heated by the exhaust gas in the evaporator. This design enables thorough utilization of the exhaust gas. The T-S diagram of this WHR system is shown in Fig. 2.

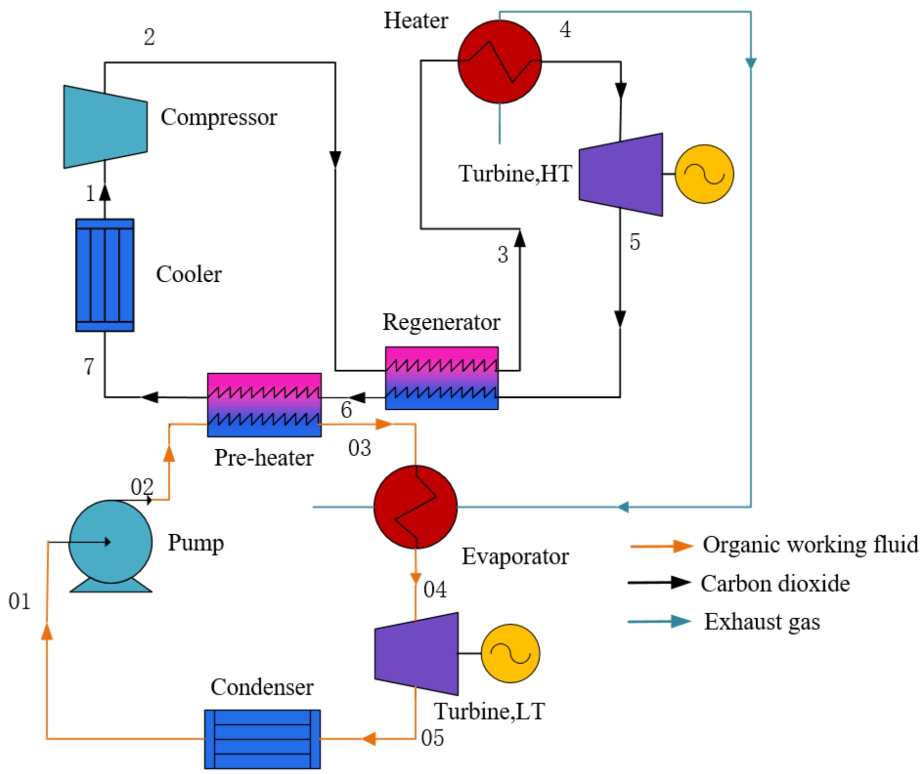

Fig. 1 Schematic diagram of RSCBC/ORC dual-loop cycle

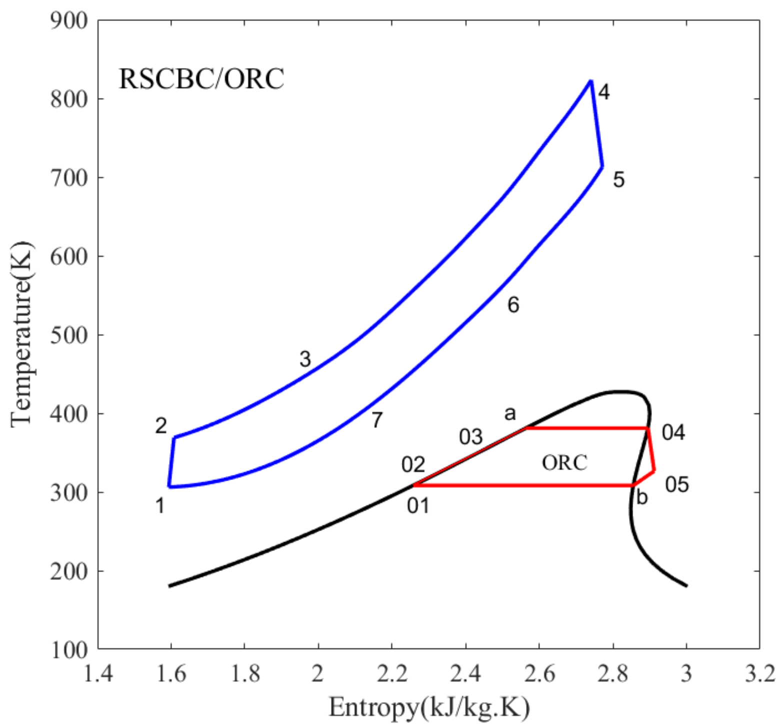

Fig. 2 T-S diagram of the RSCBC/ORC dual-loop cycle

3 Model design and validation

A program developed based on MATLAB and the REFPROP database is adopted to analyze the thermodynamic performance of the system. REFPROP is a reference fluid thermodynamic and transport properties database, which implements reference equations of state for many refrigerants and can be used to calculate all fluid properties [29].

3.1 Thermodynamic model

The following assumptions are applied for modelling:

(1) The whole system is operated at a steady state condition;

(2) Changes in the kinetic and potential energies of the fluids are negligible;

(3) Both heat loss and pressure drops in the pipelines and heat exchangers are negligible;

(4) The temperature of the exhaust gas is higher than the acid dew point after heat transfer, and the acid dew point is assumed to be 120°C.

The following thermodynamic modelling is based on the first and the second law of thermodynamics:

HT cycle:

1-2 is the compression process in the compressor:

$$\eta_{comp} = \frac{h_{2,s} - h_1}{h_2 - h_1} \tag{3}$$

$$W_{comp} = m_{co_2}(h_2 - h_1) \tag{4}$$

2-3 and 5-6 are the heat recovery processes in the regenerator:

$$h_3 - h_2 = h_5 - h_6 \tag{5}$$

$$\varepsilon_{rec} = \frac{T_5 - T_6}{T_5 - T_2} \tag{6}$$

3-4 is the endothermic process in the heater:

$$Q_{in,HT} = m_{co_2}(h_4 - h_3) \tag{7}$$

4-5 is the expansion process in the turbine:

$$W_{tur,HT} = m_{co_2}(h_4 - h_{5,s})\eta_{tur,HT} \tag{8}$$

6-7 is the heat transfer process between the HT cycle and the low temperature (LT) cycle:

$$Q_{exc} = m_{co_2}(h_6 - h_7) \tag{9}$$

7-1 is the cooling process in the cooler:

$$Q_{cool} = m_{co_2}(h_7 - h_1) \tag{10}$$

LT cycle:

01-02 is the compression process in the pump:

$$\eta_{pump} = \frac{h_{02,s} - h_{01}}{h_{02} - h_{01}} \tag{11}$$

$$W_{pump} = m_f(h_{02} - h_{01}) \tag{12}$$

02-03 is the heat transfer process in the pre-heater:

$$Q_{in,LT1} = m_f(h_{03} - h_{02}) = m_{co_2}(h_6 - h_7) \tag{13}$$

03-04 is the endothermic process in the evaporator:

$$Q_{in,LT2} = m_f(h_{04} - h_{03}) \tag{14}$$

04-05 is the expansion process in the turbine:

$$W_{tur,LT} = m_f(h_{04} - h_{05,s})\eta_{tur,LT} \tag{15}$$

05-01 is the condensation process in the condenser:

$$Q_{cond} = m_f(h_{05} - h_{01}) \tag{16}$$

The net power output of the dual-loop cycle:

$$W_{net} = (W_{tur,HT} - W_{comp}) + (W_{tur,LT} - W_{pump}) \tag{17}$$

The total heat absorbed by the dual-loop cycle:

$$Q_{in} = Q_{in,HT} + Q_{in,LT2} \tag{18}$$

The energy efficiency of the dual-loop cycle:

$$\eta_{th} = W_{net}/Q_{in} \tag{19}$$

Because kinetic and potential energies are neglected in this system, the incomplete equilibrium state is selected as the reference state. Only physical exergy is considered for exergetic analysis.

$$E = E_{ph} = m[(h - h_0) - T_0(s - s_0)] \tag{20}$$

The total exergy input of the dual-loop cycle:

$$E_{in} = E_{fin} - E_{final} \tag{21}$$

Here, E_{fin} is the exergy of the exhaust gas at the beginning, and E_{final} is the exergy of the exhaust gas after two heat exchangers.

The exergy efficiency of the dual-loop cycle:

$$\eta_{ex} = W_{net}/E_{in} \tag{22}$$

The main parameters of the dual-loop cycle and organic working fluids are shown in Table 3 and Table 4, respectively.

Table 3 Main parameters of the dual-loop cycle

Parameters	value
Turbine efficiency in HT cycle (%)	93[30]
Compressor efficiency in HT cycle (%)	89[30]
Recuperative ratio (%)	95[30]
Pinch point temperature difference in evaporator and heater (K)	30
Pinch point temperature difference in other heat exchangers (K)	5
Pump efficiency in LT cycle (%)	70[27]
Turbine efficiency in LT cycle (%)	80[27]

Table 4 Main properties of different working fluids.

Working fluid	Molecular mass	Critical temperature (℃)	Critical pressure (MPa)	Safety group	ODP	GWP
CO_2	44.01	30.98	7.38	A1	0.000	1
R600	58.12	152.0	3.80	A3	0.000	~20
R601	72.15	196.6	3.37	A3	0.000	~20
R601a	72.15	187.2	3.38	A3	0.000	~20
R601b	72.15	160.6	3.20	-	0.000	~20
R1233zd(E)	130.5	165.6	3.57	A1	0.000	4.5
R245ca	134.05	174.4	3.93	-	0.000	726

3.2 Model validation

Because there is no published literature about such a RSCBC/ORC dual-loop cycle, the established RSCBC and ORC need to be independently verified. Table 5 indicates that the efficiency error for RSCBC is 2.25%, whereas that for ORC ranges from 0.05% to 7.16% mainly because of the different versions of MATLAB and REFPROP, along with the differences in pinch point temperatures and the degree of superheat. These results demonstrate that the simulation results of both RSCBC and ORC agree well, thus providing a basis for using the present combined cycle model for further analysis of the performance of the proposed system.

Table 5 Comparison of the present calculated results with the published literature

Cycle	Working fluid	Reference	Energy efficiency in reference	Energy efficiency calculated	Error
RSCBC	CO_2	Manente [22]	36.87%	36.04%	-2.25%
ORC	Benzene	Vaja[31]	19.86%	19.85%	-0.05%
	R11		16.58%	16.11%	-2.83%
	R113		8.52%	7.91%	-7.16%

4 Results and discussion

Based on the verified combined cycle model, the thermodynamic performance of the proposed WHR system will be analyzed from three aspects including the selection of working fluids, the matching of engine conditions, and the optimization of cycle parameters in the following sections.

4.1 Selection of working fluids in organic Rankine cycle

With respect to the Rankine cycle, the properties of the working fluids significantly influence cycle performance. According to the slope of the saturated vapor line in the T-S diagram, the organic working fluids can be classified into three categories: dry fluid, isentropic fluid, and wet fluid [32]. Dry and isentropic fluids are preferred as low or medium temperature heat sources because they can avoid the occurrence of liquid hammer in the expansion process without any degree of superheat. Furthermore, the security, ODP, GWP, and other parameters of working fluids also need to be considered. Based on the above-mentioned factors, R600, R601, R601a, R1601b, R245ca and R1233zd(E) are selected for performance comparison to obtain the most suitable working fluid based on the thermodynamic performance of the dual loop cycle.

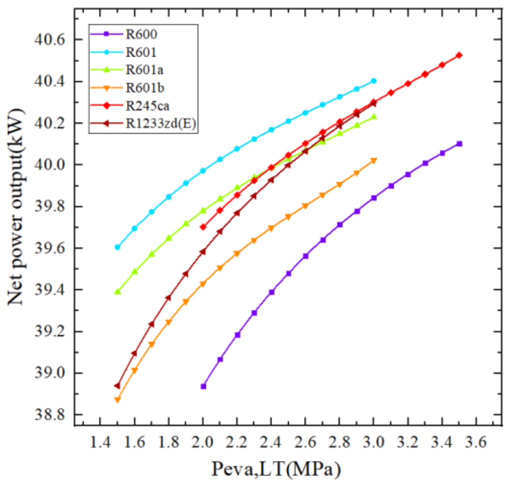

Fig. 3 (a) Changes in net power output with evaporating pressure in the LT cycle

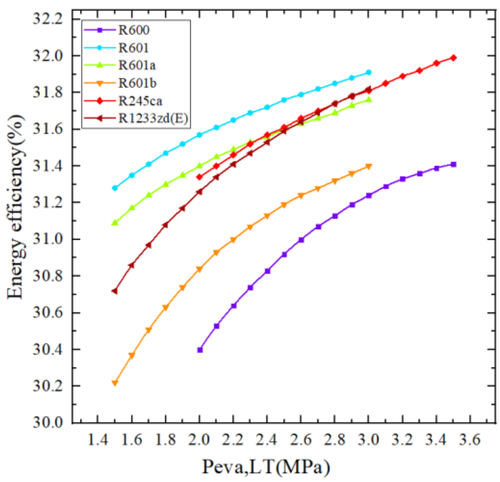

Fig. 3 (b) Changes in energy efficiency with evaporating pressure in the LT cycle

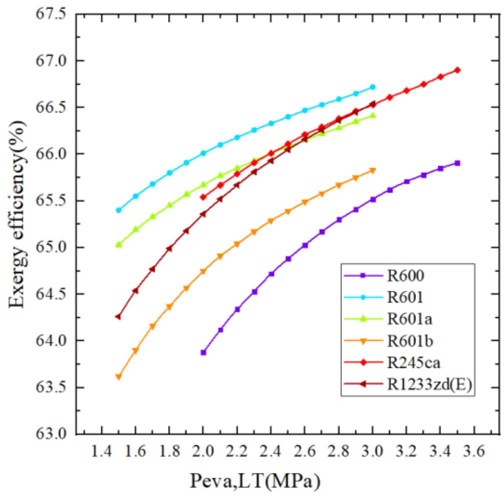

Fig. 3 (c) Changes in exergy efficiency with evaporating pressure in the LT cycle

In this part, the engine speed and torque are fixed to 1500 rpm, 1600 N·m, respectively. The evaporating pressure in the LT cycle varies while the other parameters are fixed. With respect to the HT cycle, $T_{min,HT}$ =32 ºC, $P_{min,HT}$ = 7.45 MPa, and $T_{max,HT}$ = 430 ºC. As shown in Fig. 3, the net power output, energy and exergy efficiencies of all the selected working fluids all increase with increase in evaporating pressure $P_{eva,LT}$ in the LT cycle. Among them, R601 and R600 present the maximum and minimum net power output, energy and exergy efficiencies, respectively. When $P_{eva,LT}$ is relatively low, R601 presents the best thermodynamic performance, followed by R601a, R245ca, R1233zd(E), R601b and R600. In the medium $P_{eva,LT}$, R601a, R245ca and R1233zd(E) present the similar thermodynamic performance.

4.2 Effect of engine condition

In response to the changing conditions, the thermodynamic performance of the proposed dual loop cycle is evaluated under different maximum pressures in the HT cycle and under different evaporating pressures in the LT cycle. In this part, the engine speed is fixed to 1500 rpm and the torques are 800, 1200, 1400, and 1600 N·m. The maximum pressure of the HT cycle ($P_{max,HT}$) and the evaporating pressure of the LT cycle ($P_{eva,LT}$) vary, while the other parameters are fixed. With respect to the HT cycle, $T_{min,HT}$ =32 ºC, $P_{min,HT}$ = 7.45 MPa, and $T_{max,HT}$ = 380 ºC. Comprehensively considering the security, environmental protection and thermodynamic performance, R1233zd(E) is chosen as the organic working fluid in the LT cycle.

As shown in Fig. 4, once the dual-fuel engine is operated at a steady condition, the net power output of the dual loop cycle increases with $P_{max,HT}$, and its speed of increase gradually decreases. On the one hand, both the enthalpy difference (h_4-h_5) of the expansion process in the HT cycle and that of the compression process in the HT cycle (h_2-h_1) increase as $P_{max,HT}$ increases. Furthermore, the increment in enthalpy difference of the expansion process in the HT cycle is higher than that of the compression process in the HT cycle. On the other hand, the mass flow rate of S-CO_2 (m_{co_2}) decreases with increasing $P_{max,HT}$, which results in a higher net power output. The dominant position of enthalpy difference (h_4-h_5-h_2+h_1) between the expansion and compression processes in the HT cycle is weakened, which leads to a decrease in the growth rate of the net power output. As $P_{max,HT}$ is fixed, the mass flow rate of the organic working fluid (m_f) decreases with the increase of $P_{eva,LT}$. The enthalpy difference (h_{02}-h_{01}) of the compression process in the LT cycle varies slightly and that of the expansion process in the LT cycle increases. When $P_{max,HT}$ is below 22MPa, the increment in the enthalpy difference (h_{04}-h_{05}-h_{02}+h_{01}) between the expansion and compression processes in the LT cycle is sufficient to offset the decreasing of m_f initially. As a result, the net power output of the dual loop cycle increases. When $P_{max,HT}$ is higher than 22MPa, the enthalpy difference in the LT cycle maintains the leading position first and then it is replaced by the m_f with the increase of $P_{eva,LT}$, which results in the net power output increases first and then decreases. When $P_{max,HT}$ increases simultaneously, the m_f decreases, thus the peak of the net power output appears at a lower $P_{eva,LT}$.

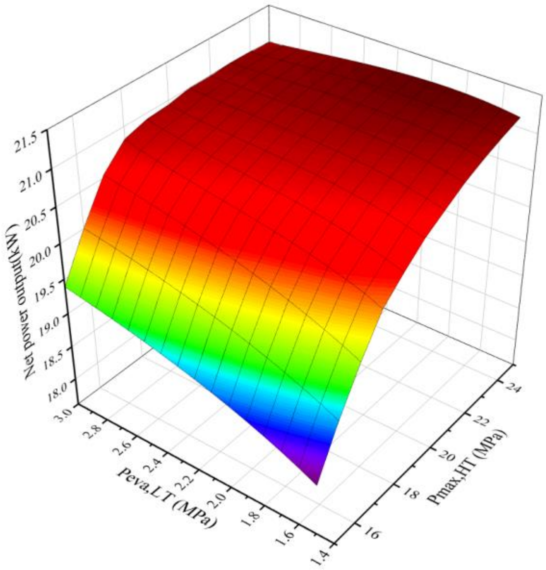

Fig.4 (a) 800N·m/1500rpm

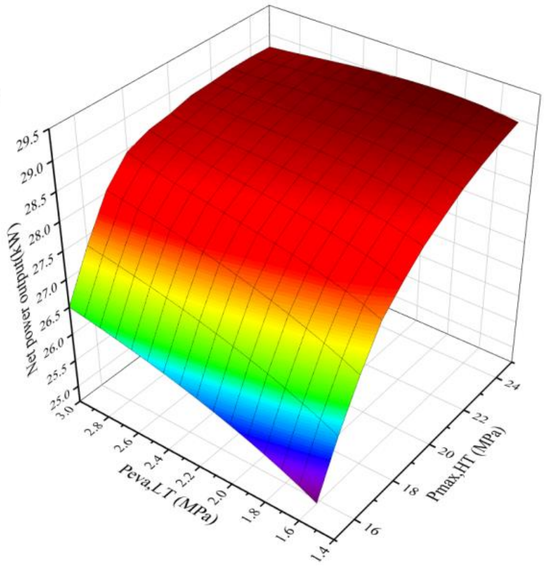

Fig.4 (b) 1200N·m/1500rpm

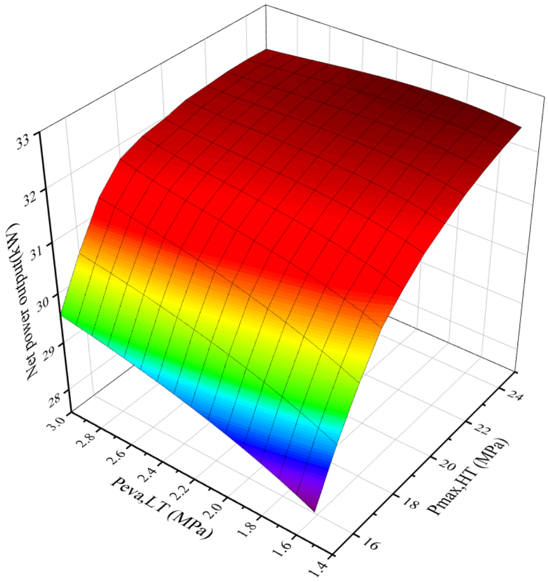

Fig. 4 (c) 1400N·m/1500rpm

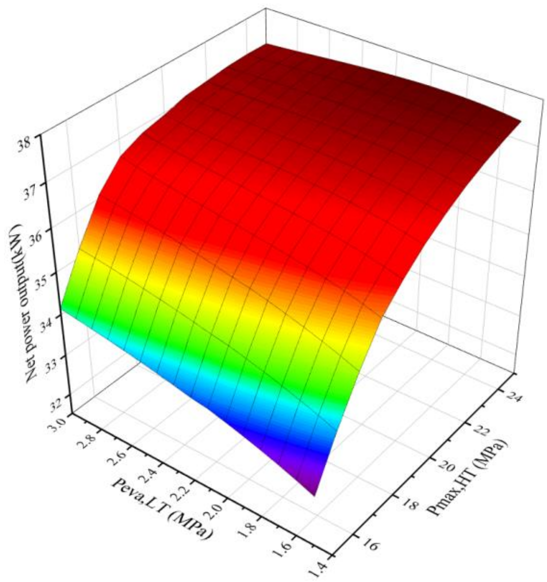

Fig. 4 (d) 1600N·m/1500rpm

Fig. 4 Net power output changes with evaporating pressure and maximum pressure under different conditions

For the dual-fuel engine, more heat is available and its quality improves because both the exhaust temperature and its mass flow rate increase with the increase of torque, as shown in Table 1. This leads to an increase in m_{co_2} and m_f based on the heat balance in the heater and evaporator. Once the parameters of the dual loop cycle are fixed, the enthalpy difference of each process remains the same and can be determined. Thus, the net power output elevates as m_{co_2} and m_f increase. Based on the above-mentioned reasons, the net power output elevates with an increase of torque when the engine speed is fixed. Selecting the net power output as the evaluation index, the optimal value of the double pressures and its maximum net power output under different conditions are shown in Table 6.

Table 6 The maximum net power output and energy efficiency corresponding to the optimal pressures

Torque	800N·m	1200N·m	1400N·m	1600N·m
$P_{max,HT}$ (MPa)	25	25	25	25
$P_{eva,LT}$ (kPa)	1900	1900	1900	1900
Net power output (kW)	21.2037	29.0446	32.4308	37.4996
Energy efficiency of engine with WHR (%)	39.69	44.88	46.68	47.81

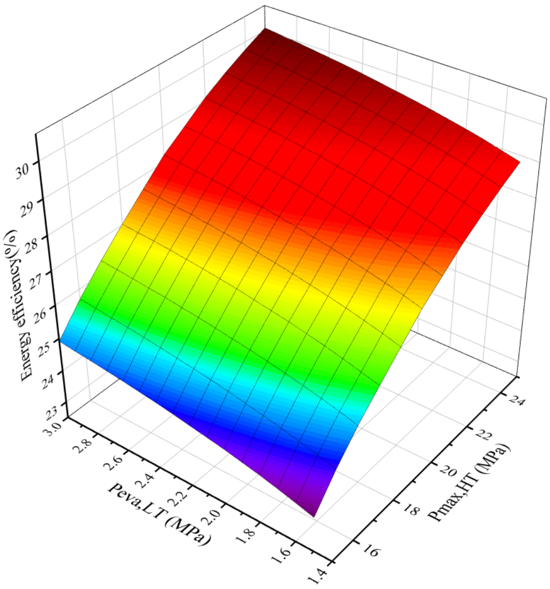

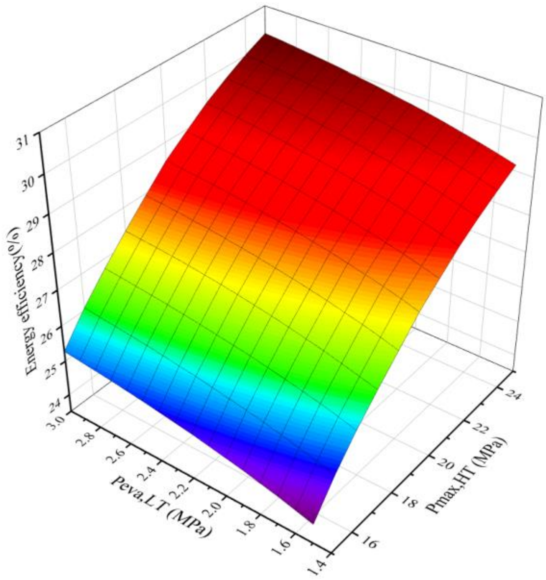

Fig. 5 (a) 800 N·m/1500 rpm Fig. 5 (b) 1200 N·m/1500 rpm

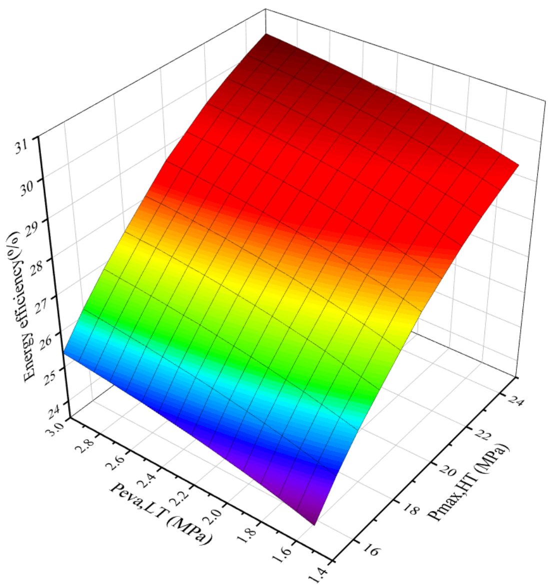

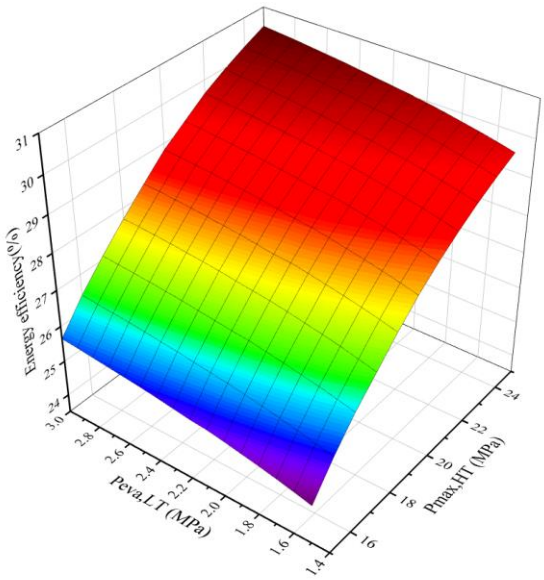

Fig. 5 (c) 1400 N·m/1500 rpm Fig. 5 (d) 1600 N·m/1500 rpm

Fig. 5 Energy efficiency changes with evaporating pressure and maximum pressure under different conditions

Fig.5 shows the effect of evaporating pressure and maximum pressure on energy efficiency. As shown in Fig. 5, when the engine is operated at a steady state condition, the energy efficiency of the dual loop cycle increases as $P_{max,HT}$ increases, which can be explained by the fact that the heat absorbed by the dual-loop cycle keeps approximately constant first and then decreases with increasing $P_{max,HT}$ while the net power output increases. The heat absorbed by the dual loop cycle stays constant with the increase of $P_{eva,LT}$ when $P_{max,HT}$ is below 18MPa, while it decreases when $P_{max,HT}$ is higher than 18MPa. Therefore, both the net power output and the heat absorption show that the energy efficiency of the dual loop cycle is elevated as $P_{eva,LT}$ increases. As the engine condition varies, the energy efficiency increases as torque increases, which is mainly caused by the increase of m_{co_2} and m_f. The maximum energy efficiencies at torques of 800, 1200, 1400, and 1600 N·m are 30.07%, 30.28%, 30.36%, and 30.50%, respectively.

As shown in Fig. 6, when the engine is running at a steady state, the exergy efficiency of the proposed WHR system increases with the increase of $P_{max,HT}$. The main reason for this phenomenon is that the net power output increases while the exergy input to the WHR system keeps constant first and then decreases.Fig.6 shows that the exergy efficiency also increases as $P_{eva,LT}$ increases. With the increase of $P_{eva,LT}$, the evaporating temperature of the LT cycle increases, which decreases the temperature difference between the organic working fluid and the heat source, including both S-CO_2 and the low temperature exhaust gas separately. Thus, the irreversibility of the pre-heater and evaporator in the LT cycle reduces, and exergy efficiency can be enhanced. As the engine conditions vary, the exhaust temperature increases with the increase of torque, which augments the temperature difference between S-CO_2 and the high temperature exhaust gas, thus increasing the irreversibility of the heater in the HT cycle and ultimately resulting in the decline of exergy efficiency. The maximum exergy efficiencies for torques of 800, 1200, 1400, and 1600 N·m are 65.48%, 64.24%, 63.77%, 62.81%, respectively.

Fig. 7 depicts the exergy loss of each component for $P_{max,HT}$ = 25 MPa and $P_{eva,LT}$ =3000 kPa under different conditions. As torque increases, the percentage of exergy loss of the heater in the HT cycle increases, while that of the evaporator in the LT cycle shows the opposite trend. In addition, the percentage of exergy loss of the regenerator and cooler fluctuates in a small range. The total exergy loss of the dual loop cycle increases as the torque increases. Under certain conditions, the heat exchangers including the evaporator, heater, cooler, condenser, regenerator, and pre-heater mainly contribute to the total exergy loss, which approximately accounts for 72% of the total exergy loss. Therefore, it is critical to reduce the irreversibility of the heat exchangers for improving exergy efficiency. Notably, the exergy loss of turbines approximately accounts for 17% to 21% of the total exergy loss, which can be explained by the relatively large pressure ratio leading to the increase of irreversibility during the non-isentropic expansion process.

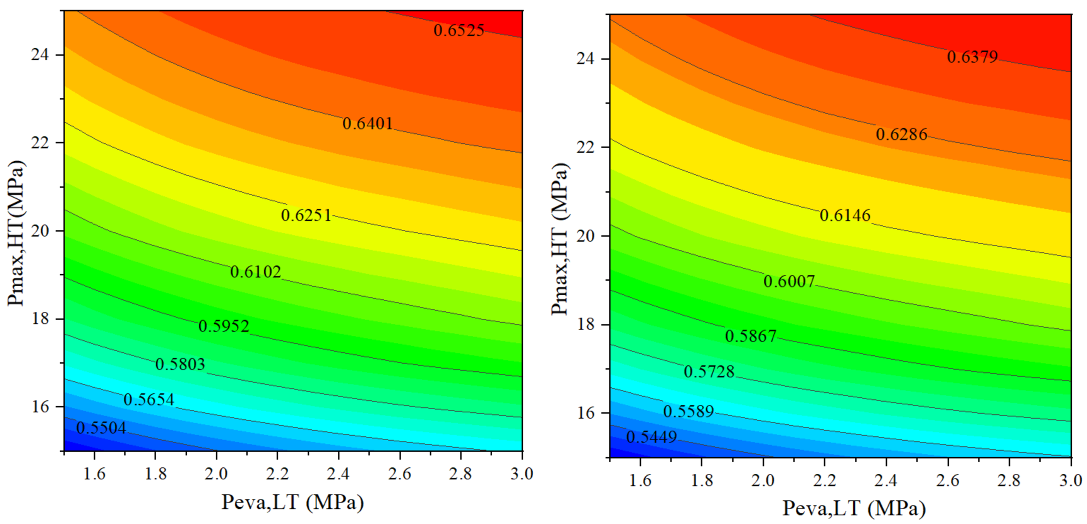

Fig. 6 (a) 800 N·m/1500 rpm Fig. 6 (b) 1200 N·m/1500 rpm

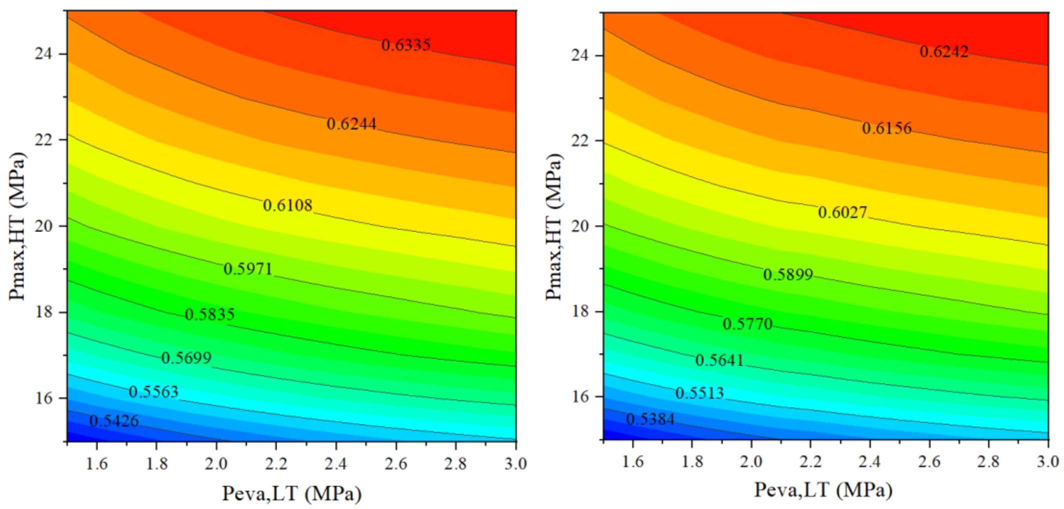

Fig. 6 (c) 1400 N·m/1500 rpm Fig. 6 (d) 1600 N·m/1500 rpm

Fig. 6 Exergy efficiency changes with evaporating pressure and maximum pressure under different conditions

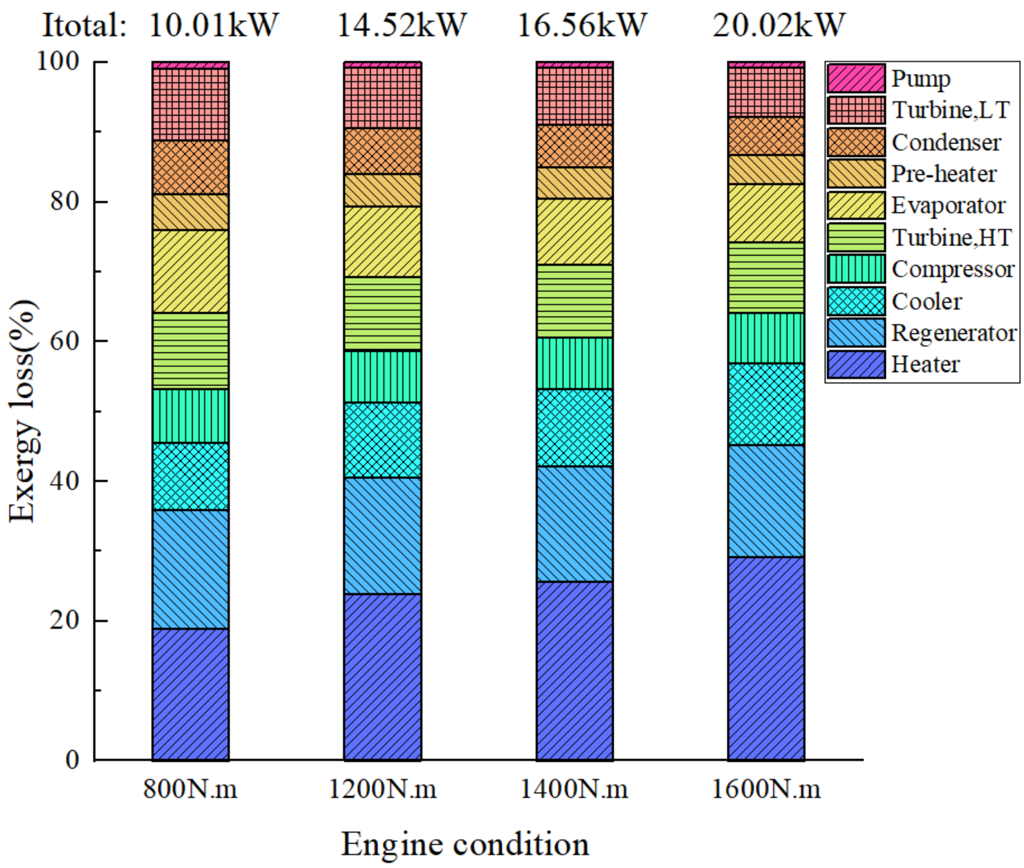

Fig. 7 Exergy loss of each component under different conditions

4.3 Effect of operation parameters of the high temperature cycle on the dual loop cycle

The effect of the turbine inlet temperature $T_{max,HT}$ in the HT cycle on thermodynamic performance is investigated on the premise that the engine speed and torque are fixed at 1500 rpm and 1600 N·m, respectively. With respect to the HT cycle, the minimum temperature, the minimum and maximum pressure are set to 32 °C, 7.45 MPa and 25 MPa, respectively. Meanwhile, the evaporating pressure in the LT cycle is set to 3000 kPa. As shown in Fig. 8, the net power output increases as $T_{max,HT}$ increases. With the increase of $T_{max,HT}$, m_{co_2} declines according to the heat balance in the heater, and the enthalpy difference of the expansion process in the HT cycle increases owing to the divergence of the isobaric line, whereas that of the compression process in the HT cycle remains constant, which results in an increase in the enthalpy difference (h_4-h_5-h_2+h_1) between the turbine and compressor in the HT cycle. The enthalpy difference in HT cycle is sufficient to compensate for the decrease of m_{co_2} , which results in the increase of the net power output of the HT cycle. In terms of the LT cycle, m_f increases as $T_{max,HT}$ increases, and the enthalpy difference (h_{04}-h_{05}-h_{02}+h_{01}) between the turbine and pump in the LT cycle remains constant, which results in an increase in the net power output of the LT cycle. The net power output of the HT and LT cycles shows that the net power output of the dual loop cycle increases. Fig. 8 shows that the energy and exergy efficiencies of the dual-loop cycle follow a similar variation trend, which can be explained by the variation of the net power output being higher than that of the heat absorption and input exergy. When $T_{max,HT}$ is 723.15 K, the net power output, energy efficiency, and exergy efficiency present the maximum value, which are 40.1706 kW, and 31.76%, 66.41%, respectively.

Fig. 9 depicts the changes in specific heat capacity of carbon dioxide with temperature under different pressures. It can be seen from Fig. 9 that the specific heat capacity of carbon dioxide changes greatly near the pseudo-critical point and decreases gradually away from the pseudo-critical point. Besides, its peak decreases gradually with the increase of pressure. As shown in Fig. 10, the net power output, energy and exergy efficiencies of the dual loop cycle are also influenced by the minimum temperature $T_{min,HT}$ and minimum pressure $P_{min,HT}$ in the HT cycle. Fig. 10(a) shows that when $P_{min,HT}$ is below 7.7MPa, the net power output decreases as $T_{min,HT}$ increases, whereas the net power output increases first and then decreases when $P_{min,HT}$ is higher than

7.7MPa. On the one hand, both m_{co_2} and m_f increase as $T_{min,HT}$ increases, and then the net power output in the LT cycle increases. On the other hand, the enthalpy difference of the compressor in the HT cycle increases, while that of the turbine in the HT cycle remains constant with the increase of $T_{min,HT}$.

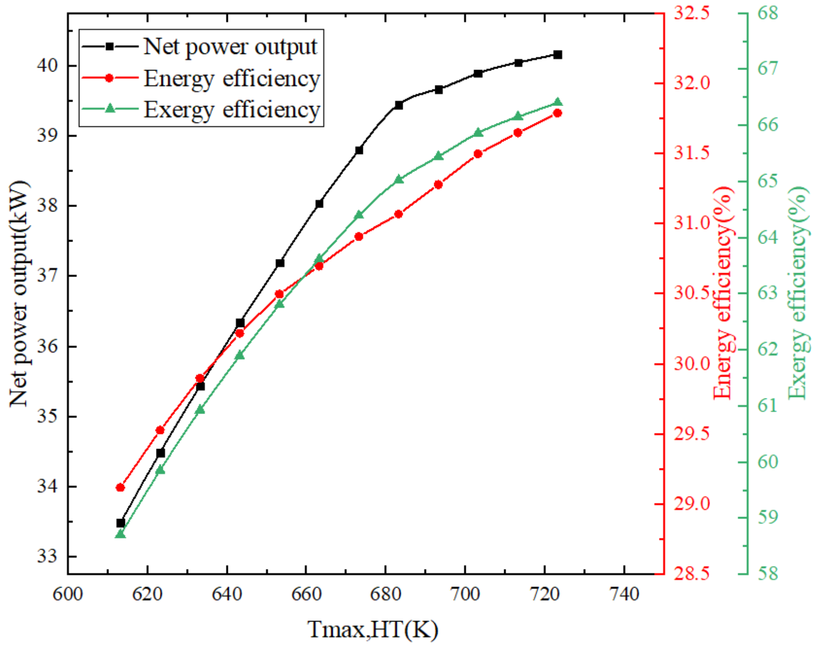

Fig. 8 Influence of turbine inlet temperature $T_{max,HT}$ in the HT cycle

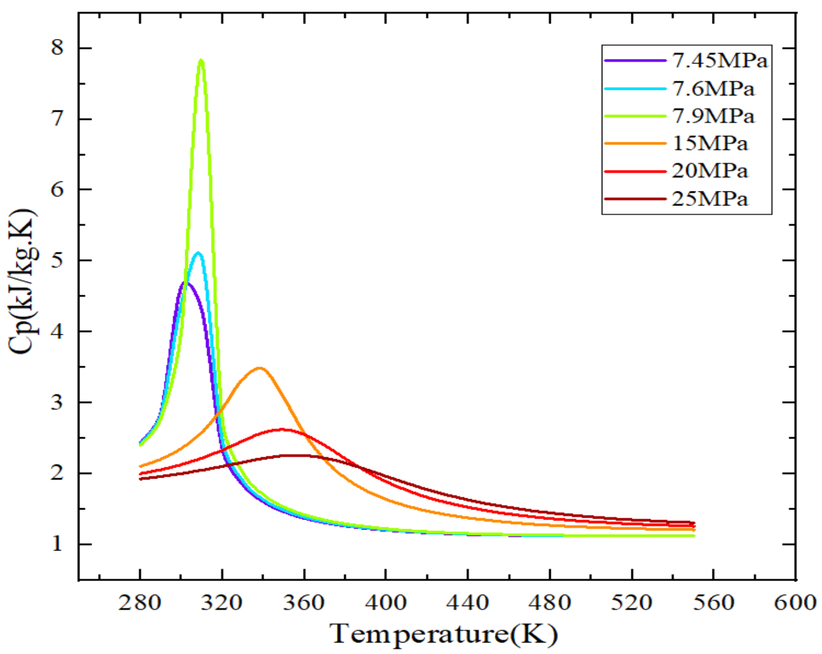

Fig. 9 Changes in specific heat capacity of carbon dioxide

Therefore, the net power output in the HT cycle declines with the synthetic effect of mass flow rate and enthalpy difference. The net power output in the HT and LT cycles determines the net power output of the dual loop cycle. Besides, Fig. 10(a) shows that the net power output slightly fluctuates with increasing $P_{min,HT}$, which can be explained by the fact that the variation of specific heat capacity of carbon dioxide, the net power output in HT cycle increases first and then decreases when $T_{min,HT}$ varies from 304.15K to 306.15K, then it increases when $T_{min,HT}$ is higher than 306.15K. And the net power output in LT cycle decreases simultaneously with increasing $P_{min,HT}$. As shown in Fig.10(b), the energy efficiency increases generally with the increasing $T_{min,HT}$ and the decreasing $P_{min,HT}$. Meanwhile, it fluctuates slightly because the heat absorbed varies greatly near the pseudo-critical point. The input exergy has the similar trend with the heat absorbed, which results in the exergy efficiency changes with $T_{min,HT}$ and $P_{min,HT}$, as shown in Fig.9(c). Different layouts with R1233zd(E) as the working fluid in LT cycle are compared in Table 7.

Table 7 Comparison with different layouts with R1233zd(E) as the working fluid with the engine running at 1500 rpm and1600 N·m

Parameters	Engine without WHR	Engine with RSCBC	Engine with RSCBC/ORC
Net power output(kW)	251.1	281.47	291.88
Overall efficiency(%)	41.6	46.63	48.38
BSFC(g/kW·h)	178.8	159.48	153.80

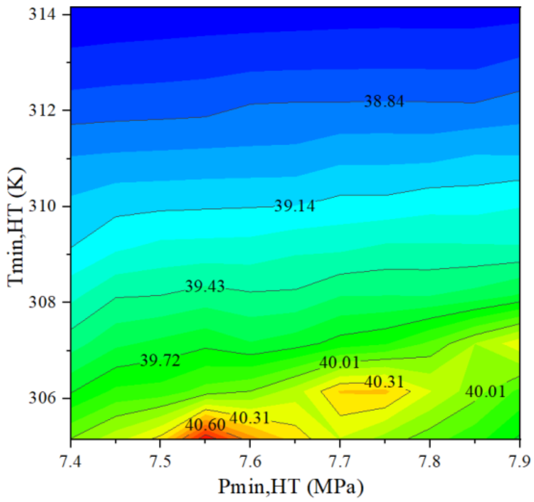

Fig. 10 (a) Changes in net power output with $T_{min,HT}$ and $P_{min,HT}$

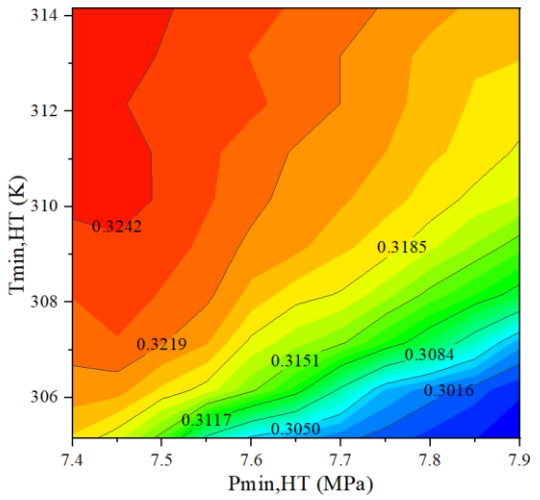

Fig. 10 (b) Changes in energy efficiency with $T_{min,HT}$ and $P_{min,HT}$

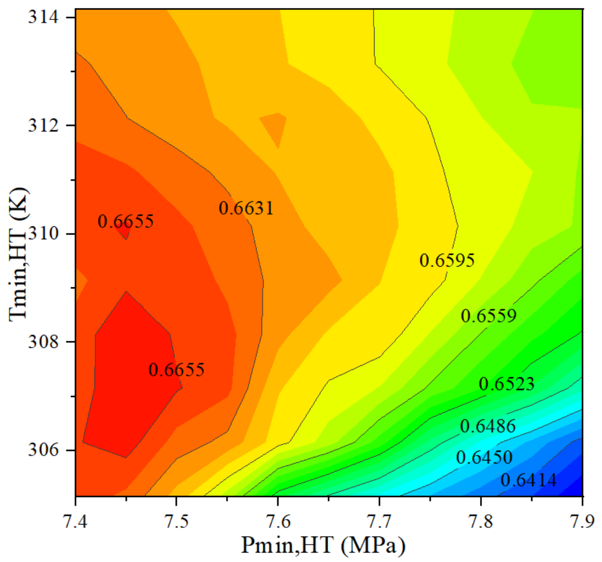

Fig. 10 (c) Changes in exergy efficiency with $T_{min,HT}$ and $P_{min,HT}$

5. Conclusion

In this paper, SCBC and ORC are adopted as the HT cycle and the LT cycle for WHR of a diesel/natural gas dual-fuel engine, respectively. The combination of these two cycles leads to thorough WHR of the dual-fuel engine via cascade utilization of energy according to temperature. Three main aspects including the matching of engine conditions, the optimization of cycle parameters, and the selection of working fluids are investigated to analyze the thermodynamic performance of the proposed dual-loop cycle. The main conclusions are as follows:

(1) The net power output of all the selected organic working fluids increases with the increasing evaporating pressure $P_{eva,LT}$ in the LT cycle. The maximum net power output, energy and exergy efficiencies of the dual loop cycle are obtained by adopting R601.

(2) At a fixed speed of 1500 rpm, the net power output of the dual loop cycle increases as torque increases. Furthermore, the net power output of the dual-loop cycle increases with the increase of the $P_{max,HT}$, and it increases with increasing $P_{eva,LT}$ when $P_{max,HT}$ is below 22MPa, while it increases first and then decreases when $P_{max,HT}$ is higher than 22MPa. Furthermore, the energy and exergy efficiencies increase with the increase of $P_{eva,LT}$ and $P_{max,HT}$.

(3) A comparison of the exergy losses of each component shows that the heat exchangers account for 72% of the total exergy loss. Therefore, reducing the irreversibility of the heat exchangers is essential for improving exergy efficiency. Notably, the exergy loss of turbines is approximately 17% to 21%, which can be explained by the relatively large pressure ratio that leads to the increment of irreversibility during the non-isentropic expansion process.

(4) The net power output, energy and exergy efficiencies of the proposed WHR system all increase with the increasing $T_{max,HT}$. And the net power output decreases as $T_{min,HT}$ increases when $P_{min,HT}$ is below 7.7 MPa, whereas it increases first and then decreases when $P_{min,HT}$ is higher than 7.7MPa. Furthermore, the net power output

slight fluctuates with increasing $P_{min,HT}$ because of the variation of specific heat capacity of carbon dioxide.

(5) The maximum net power output by adopting R1233zd(E) as the working fluid is 40.88kW, which shows improvement of the engine power output by 6.78%.

Acknowledgements

This work was supported by Natural Science Foundation of China (51865002, 51666007), Guangxi Key Laboratory of Manufacturing System & Advanced Manufacturing Technology (No. 7-259-05S002) and EPSRC (EP/N020472/1) in the United Kingdom.

Nomenclature

Abbreviations

ORC	organic Rankine cycle
SBC	supercritical Brayton cycle
SCBC	supercritical carbon dioxide Brayton cycle
TCBC	transcritical carbon dioxide Brayton cycle
RSCBC	regenerative supercritical carbon dioxide Brayton cycle
SCRBC	supercritical carbon dioxide recompression Brayton cycle
WHR	waste heat recovery
HT cycle	high temperature cycle
LT cycle	low temperature cycle

Symbols

η	efficiency
ε	recuperative ratio
s	specific entropy (kJ/kg)
h	specific enthalpy (kJ/kg)
m	mass flow rate (kg/s)
E	exergy (kW)
T	temperature (K)
Q	heat (kW)
W	work (kW)

Subscripts

HT	high temperature

LT	low temperature
comp	compression
tur	turbine
exc	exchanger
rec	recuperator
cond	condensation
cool	cooler
th	thermal
ph	physical
ex	exergy
in	inlet
max	maximum
min	minimum

Reference

[1] Xiong Q, Yeganehb MM, Yaghoubib E, Asadic A, Doranehgard MH, Hong K. Parametric investigation on biomass gasification in a fluidized bed gasifier and conceptual design of gasifier. Chemical Engineering & Processing: Process Intensification.2018;127:271-291.

[2] Thurairaja K, Wijewardane A, Jayasekara S, Ranasinghe C.Working Fluid Selection and Performance Evaluation of ORC. Energy Procedia.2019;156:244-248.

[3] Scaccabarozzi R, Tavano M, Invernizzi CM, Martelli E. Comparison of working fluids and cycle optimization for heat recovery ORCs from large internal combustion engines. Energy.2018;158:396-416.

[4] Abadi GB, Kim KC. Investigation of organic Rankine cycles with zeotropic mixtures as a working fluid: Advantages and issues. Renewable and Sustainable Energy Reviews. 2017;73:1000-1013.

[5] Braimakis K, Karellas S. Energetic optimization of regenerative Organic Rankine Cycle (ORC) configurations. Energy Convers Manage.2018;159:353-370.

[6] Hanlon M. BMW unveils the turbosteamer concept [EB/OL]. <http://www.gizmag.com/go/4936/.2005>.

[7] Li J, Liu Q, Ge Z, Duan Y, Yang Z. Thermodynamic performance analyses and optimization of subcritical and transcritical organic Rankine cycles using R1234ze(E) for 100-200 ℃ heat sources. Energy Convers Manage. 2017;149: 140-154.

[8] Mohammadkhani F, Yari M. A 0D model for diesel engine simulation and employing a transcritical dual loop Organic Rankine Cycle (ORC) for waste heat recovery from its exhaust and coolant: Thermodynamic and economic analysis. Applied Thermal Engineering.2019;150:329-347.

[9] Wang T, Gao N, Zhu T. Investigation on the optimal condensation temperature of supercritical organic Rankine cycle systems considering meteorological parameters. Energy Convers Manage.2018;174:54-64.

[10] Schuster A, Karellas S, Aumann R. Efficiency optimization potential in supercritical Organic Rankine Cycles. Energy.2010;35:1033-1039.

[11] Moloney F, Almatrafi E, Goswami DY. Working fluid parametric analysis for regenerative supercritical organic Rankine cycles for medium geothermal reservoir temperatures. Energy Procedia.2017;129: 599-606.

[12] Braimakis K, Preißinger M, Brüggemann D, Karellas S, Panopoulos K. Low grade waste heat recovery with subcritical and supercritical Organic Rankine Cycle based on natural refrigerants and their binary mixtures. Energy.2015;88:80-92.

[13] Zheng J, Wang J, Zhao Z, Wang D, Huang Z. Effect of equivalence ratio on combustion and emissions of a dual-fuel natural gas engine ignited with diesel. Applied Thermal Engineering.2019;146:738-751.

[14] Feher EG. The supercritical thermodynamic power cycle. Energy Convers.1968;8:85-90.

[15] Angelino G. Carbon dioxide condensation cycles for power production. J Eng Power.1968;90(3):287-95.

[16] Crespia F, Gavagnina G, Sáncheza D, S. Martínez G. Supercritical carbon dioxide cycles for power generation: A review. Appl Energy.2017; 195:152-183.

[17] Li M, Zhu H, Guo J, Wang K, Tao W.The development technology and applications of supercritical CO_2 power cycle in nuclear energy, solar energy and other energy industries. Applied Thermal Engineering.2017;126:255-275.

[18] Zhu H, Wang K, He Y. Thermodynamic analysis and comparison for different direct-heated supercritical CO_2 Brayton cycles integrated into a solar thermal power tower system. Energy.2017;140:144-157.

[19] Sarkar J. Second law analysis of supercritical CO_2 recompression Brayton cycle. Energy.2009;34:1172-1178.

[20] Kim S, Cho Y, Kim MS, Kim M.Characteristic and optimization of supercritical CO2 recompression power cycle and the influence of pinch point temperature difference of recuperators. Energy. 2018;147;1216-1226.

[21] Park JH, Park HS, Kwon JG, Kim TH, Kim MH. Optimization and thermodynamic analysis of supercritical CO_2 Brayton recompression cycle for various small modular reactors. Energy.2018;160:520-535.

[22] Manente G, Lazzaretto A. Innovative biomass to power conversion systems based on cascaded supercritical CO_2 Brayton cycles. Biomass And Bioenergy.2014;69:155-168.

[23] Wang X, Dai Y. Exergoeconomic analysis of utilizing the transcritical CO2 cycle and the ORC for a recompression supercritical CO2 cycle waste heat recovery: A comparative study. Applied Energy.2016;170:193-207.

[24] Akbari AD, M.S. Mahmoudi S. Thermoeconomic analysis & optimization of the combined supercritical CO_2 (carbon dioxide) recompression Brayton/organic Rankine cycle. Energy.2014;78:501-512.

[25] Singh H, Mishra RS. Performance analysis of solar parabolic trough collectors driven combined supercritical CO2 and organic Rankine cycle. Engineering Science and Technology, an International Journal.2018;21:451-464.

[26] Song J, Li X, Ren X, Gu C.Performance improvement of a preheating supercritical CO_2 (S-CO_2) cycle based system for engine waste heat recovery. Energy Conver Manage 2018;161:225-233.

[27] Song J, Li X, Ren X, Gu C.Performance analysis and parametric optimization of supercritical carbon dioxide(S-CO_2) cycle with bottoming Organic Rankine Cycle (ORC). Energy. 2018;143:406-416.
[28] Uusitalo A, Ameli A, Turunen-Saaresti T. Thermodynamic and turbomachinery design analysis of supercritical Brayton cycles for exhaust gas heat recovery. Energy.2019;167:60-79.
[29] Van CTS, R. Laughman C. Approximation of refrigerant properties for dynamic vapor compression cycle model. IFAC Papers On Line.2018;51(2):625-630.
[30] Calle A, Bayon A, Soo Too YC. Impact of ambient temperature on supercritical CO_2 recompression Brayton cycle in arid locations: Finding the optimal design conditions. Energy.2018;153:1016-1027.
[31] Vaja I, Gambarotta A. Internal Combustion Engine (ICE) bottoming with Organic Rankine Cycles (ORCs).Energy.2010;35:1084-1093.
[32] Qiu G. Selection of working fluids for micro-CHP systems with ORC. Renewable Energy.2012;48:565-570.